ARCHIVES

of

FOUNDRY ENGINEERING

Published quarterly as the organ of the Foundry Commission of the Polish Academy of Sciences

ISSN (1897-3310)
Volume 7
Issue 1/2007
47 – 52

9/1

Continuous drive friction welding of cast AlSi/SiC$_{(p)}$ metal matrix composites

J. Wysocki [a], J. Grabian [b], W. Przetakiewicz [b]
[a] Polish Marine Service
[b] Institute of Basic Technical Sciences, Maritime Academy, Szczecin, ul. Podgórna 51/53, 70-205 Szczecin, Poland

Received 08.02.2007; Approved for print on: 12.03.2007

Abstract

Continuous drive friction welding of cast AlSi/SiC(p) metal matrix composites in systems AlSi11-AlSi9/SiC/21$_{(p)}$, AlSi9/SiC/21$_{(p)}$-AlSi9/SiC/21$_{(p)}$ AlSi11/SiC/15$_{(p)}$-AlSi11/SiC/15$_{(p)}$ have been made. Examination of welds microstructure revealed that during friction welding process three different zones of size and distribution reinforced particles in the metal matrix appeared. Discernible effect of friction welding parameters on the microstructure matrix has been noticed. Subsequent hardness tests confirmed changes in matrix microstructure and influence particles redistribution on the weld mechanical properties.

Keywords: friction welding, cast AlSi/SiC$_{(p)}$ composites, reinforced distribution, hardness profile, matrix structure

1. Introduction

The development of technical spheres such as: electronic, automobile, aeronautical industry or ship building industry are associated with continuous searching for materials with low density, low specific gravity, high stiffness and specific strength, materials which preserve tensile and compression strength at high temperature. Aluminum matrix composites are materials which may be considered to offer better strength, wear resistance and stiffness when compared to conventional aluminum alloys. Important virtue of particle reinforced metal matrix composites is relative ease and economy of fabrication by conventional processing. However, the use of these materials in a wide range of industry is limited by low fracture toughness, ductility and problems with poor weldability, particularly by conventional fusion welding techniques [1].

However, dissimilar physical and chemical proportions of metal matrix and ceramic reinforced phase make this type material difficult to weld. To above mentioned engineering materials belong aluminum-base metal matrix composites cast alloy AlSi contained SiC particles. In order to obtain similar physico-chemical weld characteristic to parent material two basic conditions have to be fulfilled. The first, lack or low intensity harmful chemical reactions at interface metal matrix-ceramic phase which subsequently reducing mechanical proportions. The Second, preserve disruption of continuity and reinforced code the welding zone [2].

It is well established that joining techniques such as: TIG welding [3], MIG welding [4], electron beam welding or laser beam welding [5] have a lot of limitation which influent on quality of joint. First of all, high arc energy causes degradation of ceramic particles and changes reinforcement distribution in the dendrite arms during solidification of the molten pool. For this reason, welding procedure requires to reduce heat input energy, to limit the amount of molten material, time and temperature contact between matrix alloy and ceramic particles but more important are interfacial reaction between the ceramic reinforcement and the molten matrix alloy, resulting in unstable aluminum carbide and free silicon. Al_4C_3 is brittle, weak and unstable in wet environment causing corrosion in consequence of rapid hydrolysis [6].

Because in the continuous friction drive welding doesn't follow melting parent material, it is very promising joining method for aluminum base metal matrix composites. It is solid-state welding process in which combination series of physical phenomena, such as friction heat, plastic deformations, heat and cooling cycles and changes in the solid state take part. Appropriate force applied in axial direction makes friction contact and produces plastic deformation between two surfaces. Nearly 90% of the energy accommodated in plastic deformation is converted into heat but small part of the energy stays in specimens as strain energy. The highest temperature tip is at the beginning state friction. Temperature gradient describes heat flow in weld has the maximum magnitude at contact zone of joining surfaces. There is also concentration region of plastic deformations [7, 8]. Temperature profile in welding elements from parent material, where temperature range is nearly neglect to contact zone where temperature is proximate to melting point of aluminum matrix. Although present reinforced particles limit recrystallization process of metal matrix, the cause decrease the thermal diffusion during cooling process holding weld region at elevated temperature by extended time [7]. In this reason, task of performed continuous drive friction welding was determination microstructure changes in HAZ in comparison with parent material and degree redistribution reinforced particles in the weld.

2. Experimental procedure

2.1 Composite materials

The materials used in the present tests were $AlSi9/SiC/21_{(p)}$, with commercial designation Duralcan F3S20S, aluminum alloy AlSi11 and AlSi11 base composite reinforced by 15% SiC particles, made in Institute of Basic Technical Science, Maritime Academy Szczecin. SiC particles had not been calibrated before cast process. Preparation of the $AlSi11/SiC/15_{(p)}$ composite was proceeding as: cast aluminum alloy AlSi11 was diluted in resistant furnace, remolded in approximately 720°C and hold by half an hour. 1% of Mg has been added. SiC particles had been heated at temperature 1000 °C by 2 hours, then in proper quantity added to melt aluminum alloy with continuous stirring process. After 5 min the temperature was reduced to 580°C and stirring was continued by 15 min. Again the temperature was increased to 720°C and the mold was held by 20 min. Before, pouring to the mould the cast composite was stirred.

Workpieces were manufactured according to design as it is shown in figure 1. After machining the workpieces wer put into furnace and annealed for 150 minutes at 220°C in order to eliminate internal residual stress achieved during machining process. Before welding workpieces were cleaned and degreased.

Friction welding was performed using direct-drive welding machine ZTa-10. The joining parameters: rotation speed 1450 rpm, friction time 3.5 s, friction pressure 4 MPa in AlSi11-$AlSi9/SiC/21_{(p)}$, $AlSi9/SiC/21_{(p)}$-$AlSi9/SiC/21_{(p)}$,$AlSi11/SiC/15_{(p)}$-$AlSi11/SiC/15_{(p)}$ systems.
Metallographic preparation parent materials and welds were made as follow. $AlSi9/SiC/21_{(p)}$ and $AlSi11/SiC/15_{(p)}$ composites were cut by diamond cutter and polished with 600, 800, 1000, 1200-grid carbimet papers and finally polished using felt disk wetted by Al_2O_3 particulate suspension polishing liquid.

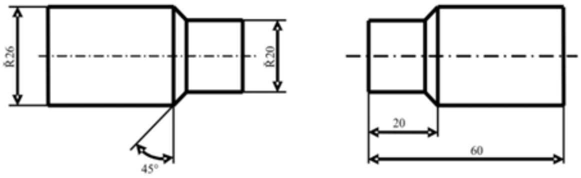

Fig. 1. The dimensions of welding workpieces

Welded workpieces which were cut perpendicularly to weld direction were prepared in the same way. Selected specimens were etched by Keller solution. Microstructures were investigated using Neophot 2 optical microscope and scanning electron microscope JOEL JSM 6100.

The Vickers hardness test was performed using HPO-250 tester with a loading of 98.07 N, a loading time 15 s. Tests were repeated four times and average values were calculate for all systems.

3. Results and discussion

3.1. Microstructure of weld metal matrix composites

Optical micrographs of $AlSi9/SiC/21_{(p)}$ and $AlSi11/SiC/15_{(p)}$ base materials are shown in figure 2a and 2b respectively.

a

b

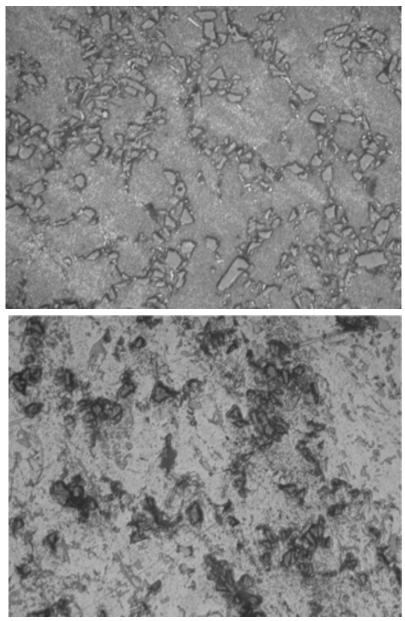

Fig. 2. Optical micrograph of base material: a) $AlSi9/SiC/21_{(p)}$, b) $AlSi11/SiC/15_{(p)}$

Microstructure of AlSi9/SiC/21$_{(p)}$ was characterized by reasonably uniform distribution of the SiC particles in the matrix without interfacial reaction products, but with light tendency to formation clusters at the grain borders. Lack of harmful reaction products type Al_4C_3 is related with quantity of Si in the matrix [9, 10]. There were no remarkable evidence hydrogen porosity or poor wetability reinforced particles by mold matrix. Small quantity of Fe-rich precipitation was noticed in matrix (fig 3). Non uniform distribution of SiC particles is the result of solidification process of aluminum base metal matrix composites [11].

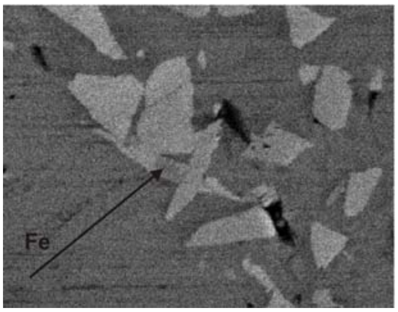

Fig. 3. Fe-rich precipitation in the AlSi9/SiC/21$_{(p)}$

Somewhat different microstructure was observed in the AlSi11/SiC/15$_{(p)}$ composite. SiC particles were uniformly distributed in matrix. Additionally, high porosity and Si blocks at SiC particles were noticed (fig. 4). Composite AlSi11/SiC/15$_{(p)}$ was not modified in order to determinate the influence of friction welding process on structural changes in the welded zone.

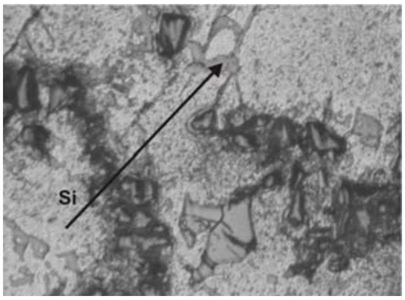

Fig. 4. Si block in the AlSi9/SiC/21$_{(p)}$

3.2. Structure of heat effect zone

As was established by Midling and Grong [7, 8], the heat affected zone (HAZ) in the friction weld of Al/SiC metal matrix composite is divided into three separate zones: the fully plasticized region, the partly deformed region and undeformed region. Figure 5 illustrates the scheme of arrangement of above mention zones.

In figure 6 are shown macroscopic pictures of produced continuous friction welds and intersection in the perpendicular direction to joined surface. System AlSi9/SiC/21$_{(p)}$-AlSi9/SiC/21$_{(p)}$ was characterized by symmetric, uniform shape of up-set collar. However, cracks parallel to weld direction appeared the outer peripheries (fig 6a). The mentioned cracks propagated across the whole up-set collar but did not rich outer surface of welded workpieces. The welds prove good alignment without any deformations in the radial direction. Axial up-setting was approximated 3.5 mm on both sides.

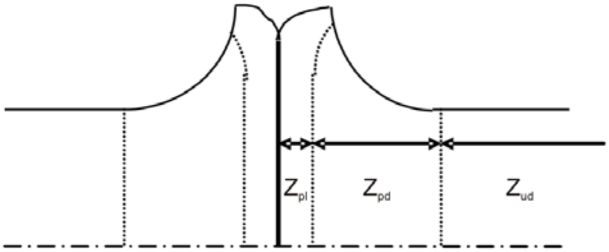

Fig. 5. Schematic illustration of the different reaction zones in the HAZ of friction welded components. Z_{pl} - fully plasticized zone, Z_{pd} – partly deformed region, Z_{ud} – undeformed region. After Midling and Grong [6].

Welds AlSi11/SiC/15$_{(p)}$-AlSi11/SiC/15$_{(p)}$ had a bit different shape of up-setting collars (fig. 6c). Their rims were rough with significant crumble away areas. These damages spread either on the surface of specimens or into the contact zone.

In figure 7a and 7b is shown weld microstructure of AlSi11-AlSi9/SiC/21$_{(p)}$. In the contact zone, SiC particles bands, which passed from metal matrix composites to unreinforced alloy are distinctly noticed (fig. 7a). To explain this behavior, the proceeding friction welding process must be taken into consideration. The beginning phase of welded surface contact can be described as large numbers of local adhesion/seizure contacts between protruding asperities and reinforcing particles which later will be sheared. The magnitude of contact pressure is conditioned by the combination of surface topography, coefficient of friction and material elastic moduli. [12].

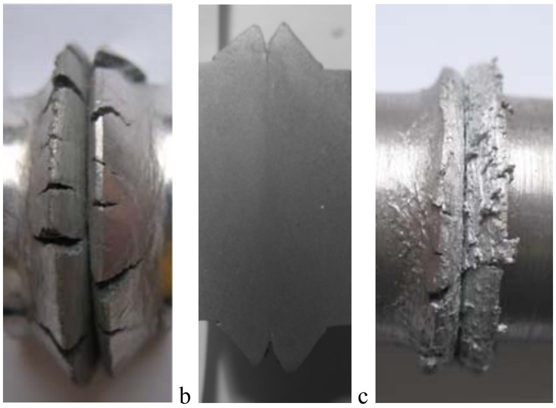

a b c

Fig. 6. Optical macrograph of: a) shape of up-set collar in AlSi9/SiC/21$_{(p)}$-AlSi9/SiC/21$_{(p)}$ system, b) weld intersection in AlSi9/SiC/21$_{(p)}$-AlSi9/SiC/21$_{(p)}$ system, c) shape of up-set collar in AlSi11/SiC/15$_{(p)}$-AlSi11/SiC/15$_{(p)}$ system.

Simultaneous destruction of this kinds of local bonds and increasing friction pressure transfer components of one material to another in both direction [8] In further process phase when parameters such as: revolutions, temperature and axial up-setting reach approximate constant value, full plasticize of welded material is ensues.

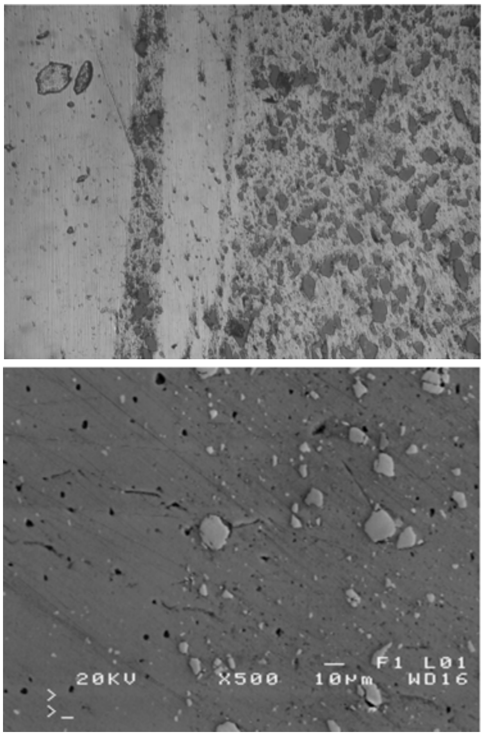

a

b

Fig. 7. Optical micrograph a) band of particles transferred from composite to unreinforced alloy in AlSi11-AlSi9/SiC/21$_{(p)}$ system, b) uniform distribution particles in contact region in AlSi11-AlSi9/SiC/21$_{(p)}$ system.

It is obvious fact that reinforced particles presents in matrix is a barrier for her plastic strains [8]. Consequently, it has bearing on specificity flow of plasticized material during its mixing, on which the biggest influence has the magnitude shear stress at higher temperature. After that, when compress force is pressured, the material with higher strength and less plasticized is pushed into direction of smaller shear strength in higher temperature [13]. Hence, presence of reinforced particles in the AlSi11 alloy in some distance from contact interface.

In presented AlSi11-AlSi9/SiC/21$_{(p)}$ system, when two substrates were brought to contact, as first the protruding points of surfaces are bonding (AlSi11-AlSi9 composite matrix and AlSi11-composite reinforced particles). In figure 7b is shown microstructure in contact region. It can be notice that a lot of SiC particles are fractured, crack and somewhere small amount decohesion matrix-reinforced was observed.

During the friction of two substrates, shear stress can cause break the coarse, primary crystal, dendrites, eutectics and Si-rich blocks in parent material [15]. As the result of above mentioned effect welded region structure which was different from the parent material was being formed.

In figure 8 (a and b) microstructures of contact region for AlSi9/SiC/21$_{(p)}$-AlSi9/SiC/21$_{(p)}$ and AlSi11/SiC/15$_{(p)}$-AlSi11/SiC/15$_{(p)}$ system respectively were shown. Under the influence of material mixing and simultaneous application of high pressure SiC particles were evenly distributed in matrix. The particles size was markedly decreased in the contact region. Two range particles size could be observed. Particles up to 2 μm, which the most probable are the result of contact of two substrates at high velocity and pressure. The present of particles of unchanged dimension and deprived fracture in the full plasticized region is the result of processes occurring in the further phase of friction welding. As mentioned earlier, the sudden increase temperature during friction two substrates causes plasticity of matrix. Further pressure of joined elements extorted plastic flow of matrix and pushes particles from partly deformed region to full plasticized region. Additionally, microstructure of full plasticized region in AlSi11/SiC/15$_{(p)}$-AlSi11/SiC/15$_{(p)}$ system in contrast to parent material was deprived of gas porosity and Si-blocks were torn and mixed.

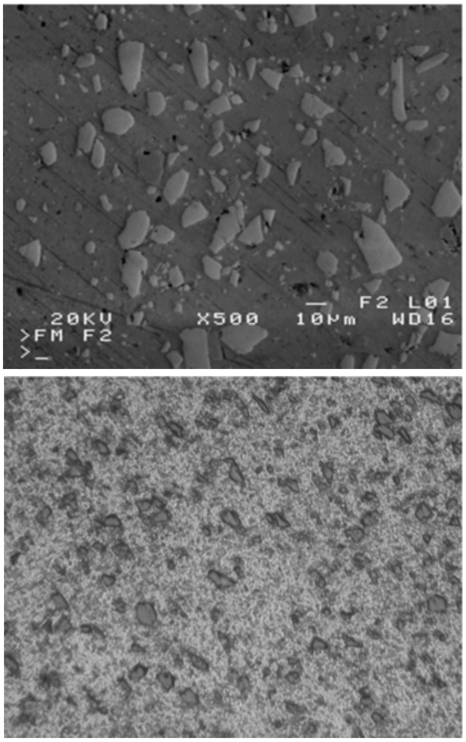

a

b

Fig. 8. Micrograph of contact region a) in AlSi9/SiC/21$_{(p)}$-AlSi9/SiC/21$_{(p)}$ system, b) AlS11/SiC/15$_{(p)}$-AlSi11/SiC/15$_{(p)}$ system.

As was mentioned earlier, HAZ in weld can be divided into three regions. Figure 9 shows structural changes in welds for AlSi9/SiC/21$_{(p)}$-AlSi9/SiC/21$_{(p)}$ and AlSi11/SiC/15$_{(p)}$-AlSi11/SiC/15$_{(p)}$ system at ¾ radius from the symmetry axis. Borderlines between regions were marked by thicken lines which had been established by observation of microstructure and hardness tests. $AlSi9/SiC/21_{(p)}$-$AlSi9/SiC/21_{(p)}$ system and $AlSi11/SiC/15_{(p)}$-$AlSi11/SiC/15_{(p)}$ system alike, microstructure of partly plasticized region was different than parent material. The reinforced particles were more evenly distributed in matrix. However, particles had feature propensity to form bents.

It is result of the fact that during friction welding process material flow is combination of axial thrust, centrifugal force and radial velocity [16].

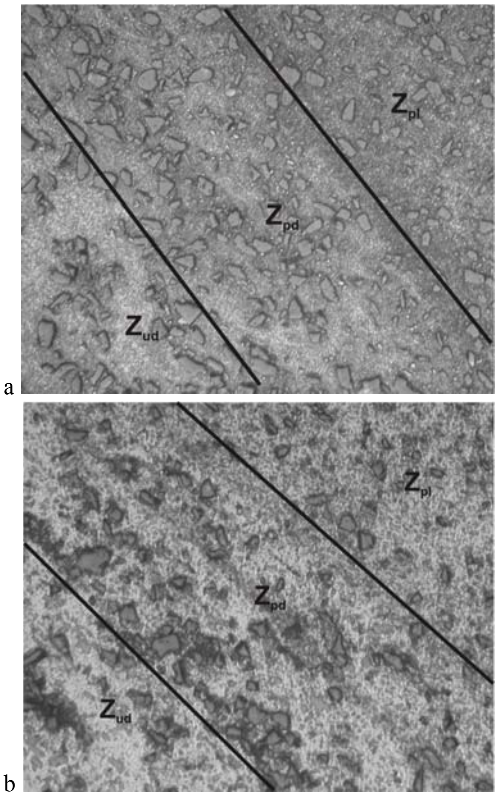

Fig. 9. Regions of microstructure changes in the HAZ: for $AlSi9/SiC/21_{(p)}$-$AlSi9/SiC/21_{(p)}$ system, b) for $AlSi11/SiC/15_{(p)}$-$AlSi11/SiC/15_{(p)}$ system

3.3. The hardness of the HAZ

The hardness tests were performed and average values were chosen for $AlSi11$-$AlSi9/SiC/21_{(p)}$, $AlSi9/SiC/21_{(p)}$-$AlSi9/SiC/21_{(p)}$, $AlSi11/SiC/15_{(p)}$-$AlSi11/SiC/15_{(p)}$ systems. Hardness coincided with microstructural changes in the HAZ. Hardness of Z_{ud} regions was similar to the parent material for all systems. Unfortunately, its value dropped drastically in the partial deformed regions on both sides. The hardness profile of plasticized regions was different in all the systems. The results of hardness tests are presented in figures 10 a-c. As it is evident from the plots, for system unreinforced alloy - metal matrix composite, hardness of full plasticized region is higher than AlSi11 alloy. As discussed earlier, it is result transferring reinforced particles from $AlSi9/SiC/21_{(p)}$ to AlSi11 during mixing materials. It proves good joining reliability.

Different hardness profiles can be observed for $AlSi9/SiC/21_{(p)}$-$AlSi9/SiC/21_{(p)}$ and for $AlSi11/SiC/15_{(p)}$-$AlSi11/SiC/15_{(p)}$ systems. In both cases drastical drop of hardness in partial plasticized regions was obtained. Accompanying element of high temperature of the HAZ is annealing effect strengthened by present slower cooling down SiC particles, whereas compared to partly deformed region hardness increased in full plasticized region was noticed. However, for $AlSi9/SiC/21_{(p)}$-$AlSi9/SiC/21_{(p)}$ systems hardness is lower than within undefomed regions. The most probably, high density reinforced particles in full plasticized region is effective an barrier for dislocation movement. Hence the conclusion, that high density SiC particles and restriction of dislocations shift must act against annealing effect and prevent the loss of hardness in full plasticized region.

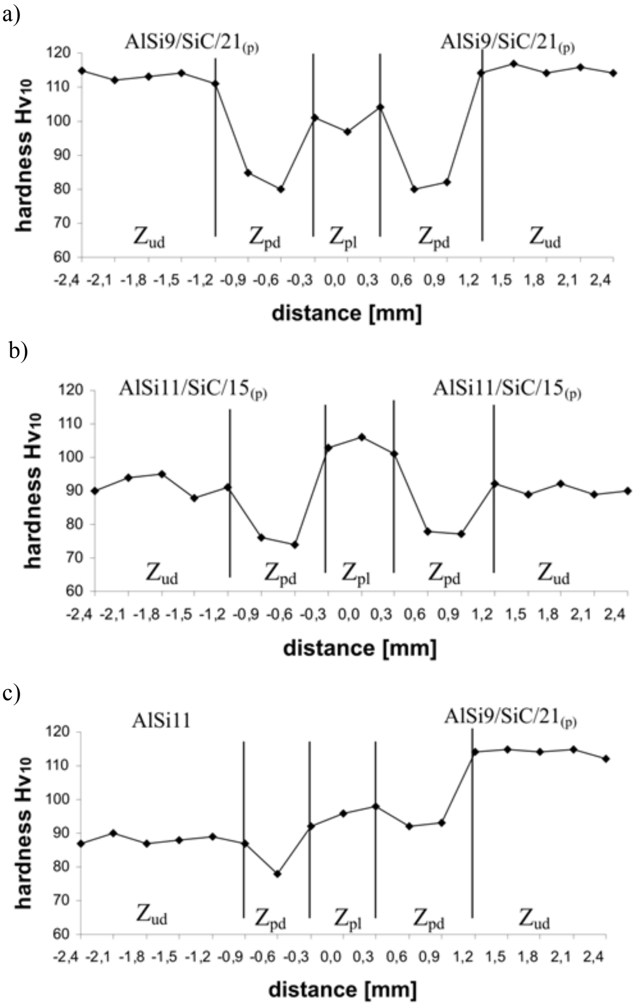

Fig. 10. The hardness profile in heat effect zone of continuous drive friction weld. a) $AlSi9/SiC/21_{(p)}$-$AlSi9/SiC/21_{(p)}$ system, $AlSi11/SiC/15_{(p)}$-$AlSi11/SiC/15_{(p)}$ system, c) $AlSi11$-$AlSi9/SiC/21_{(p)}$ system.

Unexpectedly, hardness of full plasticized region in $AlSi11/SiC/15_{(p)}$-$AlSi11/SiC/15_{(p)}$ system was higher than in the parent material. Similarly to system $AlSi9/SiC/21_{(p)}$-$AlSi9/SiC/21_{(p)}$, reduction dimension of SiC particles and their evenly distribution in matrix ensued. Additionally, under shear stress Si blocks and SiC particles clusters were broken and mixed during plastic flow. It is noticeable that in full plasticized region lacks gas porosity in contrast to $AlSi11/SiC/15_{(p)}$ which can explain hardness increase in full plasticized region.

4. Conclusions

After microstructure analysis of performed continuous drive friction welds, the following conclusions have been reached:

1. For all performed welds ($AlSi9/SiC/21_{(p)}$-$AlSi9/SiC/21_{(p)}$, $AlSi11/SiC/15_{(p)}$-$AlSi11/SiC/15_{(p)}$, AlSi11-$AlSi9/SiC/21_{(p)}$) in HAZ three regions differing in structure can be distinguish: full plasticized region, partly deformed region and undeformed region.
2. In all weld systems, partly deformed region was characterized by band distribution of reinforced particles and reduced hardness of matrix.
3. Reinforced particle transfer from composite to unreinforced alloy, likewise full plasticized region hardness increase (particularly in $AlSi11/SiC/15_{(p)}$-$AlSi11/SiC/15_{(p)}$ system), proves good mixing welded materials and weld reliability.

References

[1] W.H. Hunt, Jr : Aluminium Metal Matrix Composites Today. Material Science Forum Vols. 331-337 pp. 71-84, 2000 Trans Tech Publication, Switzerland

[2] G.G. Chernyshov, S.A. Paniczenko, T.A. Chernyshova: Welding of Metal Composites. Welding International, Vol. 17, no. 6, pp. 487-492

[3] A. Ureña, M.D. Escalera, L. Gil: Influence o interface reactions on fracture mechanisms in TIG arc-welded aluminum matrix composites. Composites Science and Technology 60 (2000) 613-622

[4] P.P. Lean, L. Gil, A. Ureña: Dissimilar welds between unreinforced AA6082 and AA6092/SiC/25p composite by pulsed-MIG arc welding using unreinforced filler alloys (Al-5Mg and Al-5Si). Journal of Materials Processing Technology 143-144 (2003) 846-850

[5] T.J. Lienert, E.D. Brandon, J.C. Lippold: Laser and electron beam welding of SiCp reinforced aluminum A-356 metal matrix composites. Scripta Metallurgica et Materialia Vol. 28, pp. 1341-1346, 1993

[6] J.K. Park, J.P. Lucas: Moisture effect on SiCp/6061 AL MMC: dissolution of interfacial Al_4C_3. Scripta Materiala (37)1997, pp. 511-515

[7] O.T. Midling, O. Grong: A Process Model For Friction welding Of Al-Mg-Si And Al-SiC Metal Matrix Composites – II. HAZ Microstructure and Strength Evolution. Acta Metallurgica Materiala, Vol.42, No.5, pp. 1611-1622, 1994

[8] O.T. Midling, O. Grong: A process model or friction welding of Al-Mg-Si alloys and Al-SiC metal matrix composites – I. HAZ temperature and strain distribution. Acta Metallurgica Materiala, Vol. 42, No.5, pp. 1595-1609, 1994

[9] A. Dolata-Grosz, M. Dyzia, J. Śledziona, J. Myalski: Influence of ceramic reinforcement kind on the solidification process of aluminum matrix. Archives of Foundry. Year 2006, Volume 6, No 22, pp. 145-150 (in polish)

[10] K. Gawdzińska, J. Grabian, A. Dolata-Grosz. Selected usable proporties of AlSi11/1H18N9T suspension composites. Archives of Foundry. Year 2006, Volume 6, No 22, pp. 145-150 (in polish)

[11] M. Dudyk: Crystallization and thermal expansion of alloys and silumine composites. Archives of Foundry. Year 2006, Volume 6, No 22, pp. 164-169 (in polish)

[12] M. Chandrasekaren, A.W. Batchelor, S. Jana: Study of the interfacial phenomena during friction surfacing of aluminum with steels. Journal of Materials Science 32 (1997) 6055-6062

[13] L.Fu, L.Y. Duan, S.G. Du: Numerical Simulation of Inertia Friction Welding Process by Finite Element Method. Welding Journal, March 2003, s. 65-70

[14] C. Malonado, T.H. North: Particle fracture in metal-matrix composite friction joints. Journal of Material Science 32 (1997) 4739-4748

[15] B. Lin, C.K. Mu, W.W. Wu, C.H. Hung: The Effect of Joint Design and Volume Fraction on Friction Welding Properties of A360/SiC(p) Composites. Welding Journal, March 1999, s.100-108

[16] T.J. Lienert, P.B. Nagy, A. Baeslack III: Ultrasonic Characterysation of Microstructure in Inertia Friction Welds on SiC-Reinforced 8009 Aluminum. Welding Journal, January 1998, s. 14-28